Robust Verification With Subsurface Fingerprint Recognition Using Full Field Optical Coherence Tomography

Kiran B. Raja[1*] Egidijus Auksorius[2*] R. Raghavendra[1*] A. Claude Boccara[2] Christoph Busch[1]
[1]Norwegian Biometrics Laboratory, NTNU Norway
[2]Institut Langevin, ESPCI ParisTech, PSL Research University, CNRS UMR 7587, Paris, France

Abstract

Fingerprint recognition has been extensively used in numerous civilian applications ranging from border control to everyday identity verification. The threats to current systems emerge from two facts that can be attributed to potential loss in accuracy due to damaged external fingerprints and attacks on the sensors by creation of an artefacts (e.g. silicone finger) simply by lifting the latent fingerprints. In the growing need for attack resistant biometric fingerprint recognition that can be operated without supervision, a new generation of sensors has been investigated, which can capture the subsurface fingerprint pattern. In this work, we explore a subsurface fingerprint imaging technique by employing a custom-built in-house Full-Field Optical Coherent Tomography (FF-OCT) sensor for capturing the subsurface fingerprint. Further, we evaluate a newly constructed database of 200 *unique fingerprint samples collected in* 2 *different sessions with* 6 *layers of fingerprint images corresponding to 6 subsurface fingerprints. We also propose a framework based on quality metrics to fuse the subsurface fingerprint images to achieve a robust verification accuracy, which has resulted in Equal Error Rate (EER) of* 0%. *We also provide an extensive set of experiments to gauge the reliability of subsurface fingerprint recognition and deduce a set of important conclusions for the path forward in FF-OCT subsurface fingerprint imaging.*

1. Introduction

Fingerprint based verification or identification of individuals has become an ubiquitous mode of access control for various applications that range from civilian border crossing controls to everyday use of smartphone unlocking. The preference towards observing the biometric fingerprint characteristic for secure access control can be largely attributed to the accuracy and reliability proven over the last decades. Added to that, the low cost factor involved in producing the fingerprint sensors has contributed in large scale deployment of fingerprint based recognition systems.

While fingerprint recognition is well adopted and used in various spheres, a number of key problems have raised concerns in the recent past. The traditional problem of cuts, abrasions and burns on the fingerprint leads to a temporal or permanent loss of the fingerprint pattern, which result in low quality fingerprints obtained with optical sensors (e.g. sensors based on frustrated total internal reflection). The problem arises when such cuts and burns lead to procuring spurious minutia points or at the very least result in a case that no minutiae are detected. In order to handle such a scenario where a particular fingerprint pattern is not observable, multiple finger instances can be employed such that one of them at-least can establish the identity claim. With regards to recently discussed threats to fingerprint based systems, attackers have demonstrated the use of lifted prints from latent fingerprints to successfully create an artefacts, which can in turn be used as presentation attack instrument. Thus the need for reliable and robust fingerprint sensors has been stressed. Such sensors are expected to: (1) Handle the challenges of disappeared external fingerprints due to any reason and, (2) Have reliable fingerprint acquisition method to determine the liveness of the fingerprint.

1.1. Related Works

A limited set of works have proposed hardware based approaches to handle failure to capture problems arising due to skin surface properties or due to the loss of the outer fingerprints as a result of injuries and also addressed presentation attacks with artefacts (e.g. silicone fingers) [2, 5, 16, 9, 15]. Multispectral imaging (MSI) is one of the subsurface techniques proposed and available commercially that generates a subsurface fingerprint image from images collected at different wavelength, illumination and polarization settings[14].

In contrast, optical coherence tomography (OCT) is able to capture subsurface in vivo images from deeper layers of the living tissue, such as a fingertip [8]. This is important since it enables imaging of the so-called *internal finger-*

*Authors have contributed equally.

prints. An image of an internal fingerprint pattern will not be impacted by cuts or abrasions since the stratum corneum, a thick skin layer on top of a finger, shields it from mechanical and other damages [10]. First, OCT has been used in fingerprint sensing domain to demonstrate presentation attack detection (a.k.a. spoof attack detection) [7] following which the first images of internal fingerprints were acquired [6]. Later images of sweat glands [12] and even blood microcirculation have been demonstrated [17, 11]. However the caveat with OCT systems that have been used for fingerprint imaging is that they have to acquire 3D data, sampled approximately equally in all the directions, before being able to reconstruct a 2D (en face) subsurface image, like that of an internal fingerprint. Unless expensive laser sources are used, the typical acquisition time for 256×256 en face image can take over 4 seconds. The fastest OCT-based system that was used for fingerprint imaging was able to acquire such image in 1 second [4]. However, the system is expensive and the associated data processing doubles the total acquisition time. Full-field OCT (FF-OCT) on the other hand is an inexpensive OCT variant that uses a camera and a spatially incoherent light source. Use of the camera allows acquiring en face image with much faster speed than possible with standard OCT systems. To this end FF-OCT based fingerprint sensors were developed working in the infrared [2] and near-infrared [3] spectral regions. The FF-OCT sensors can in principle be used to acquire the full volumetric (3D) data by translating the reference reflector in small steps between the en face images. However, instead the full volume we strategically pick only a couple of en face images recorded at different depths below the surface in order to reduce the acquisition time to a minimum. Internal fingerprints have the same topography as the external (conventional) fingerprint pattern, which is convenient since standard algorithms for minutiae extraction and fingerprint comparison can be employed, even though they might not be optimal for the captured sample. The internal fingerprint in OCT images corresponds to the viable epidermis [1] that is below the stratum corneum, although it is sometimes referred to as the papillary layer, which is intertwined with the viable epidermis and is almost at the same depth. Apart from the conventional fingerprint that is recorded from the top of the stratum corneum and apart from sweat ducts that can be recorded from the inside of the stratum corneum, a low contrast fingerprint pattern could also be captured inside the stratum corneum. This might be convenient since it relaxes the need to capture the internal fingerprint whose depth is known to change from finger-to-finger. Subsurface fingerprint is a general term used for a fingerprint acquired below the surface and we will use it here in that sense when referring to fingerprint samples acquired inside the stratum corneum or from the internal fingerprint (viable epidermis) or both and further refer it as *layers/depth*.

1.2. Contributions

Motivated by the limited works to study the biometric applicability of OCT sensors for biometric recognition, in this work we analyse the subsurface fingerprint data captured from the newly designed, in-house Full-Field Optical Coherent Tomography (FF-OCT) system comprised of a novel silicon camera [3]. The FF-OCT sensor has superior imaging and resolving ability to obtain high quality subsurface fingerprints in a reasonable amount of time (< 1 second for 6 subsurface images at different depths). Further, with the set of a large scale database consisting of 200 unique subsurface fingerprints acquired using the FF-OCT sensor, we demonstrate high recognition accuracy with subsurface fingerprints. As described above, the depth of an internal fingerprint can change from data subject to data subject and finger instance to finger instance making a reliable recognition from an internal fingerprint a challenge. In order to address this issue, in this work, we acquire a set of 6 subsurface images from different depths (in the range of $70 - 420\mu m$) in the newly constructed database. Given the range and number of images acquired, it is likely that the internal fingerprint will be captured at least in one of the images. However, in cases when the internal fingerprint is deeper than 420 μm, and thus, not recorded, a low-contrasted fingerprint from inside of the stratum corneum might be captured. Even though the internal fingerprint gives better images, when it is very deep ($> 500\mu m$), the contrast gets very low due to light absorption and scattering inside a finger. Our task was therefore to find a set of imaging depths that has the most diagnostic value in a large-scale database. Thus we present a detailed analysis of the recognition accuracy obtained from a number of different subsurface images (hereafter referred as *layers/depth*) and thereby, determine the suitability of subsurface fingerprints for reliable recognition in a large scale database. As we have a number of depth images, we also present a fusion approach to choose a set of best possible images to form a robust image whose features are further extracted for comparison. Extensive experiments are carried out using a set of newly defined protocols to evaluate the created database and to demonstrate the merits of the FF-OCT imaging for the subsurface fingerprint recognition. The key contributions of this work can be outlined as:

- Presents a new large-scale database of FF-OCT subsurface fingerprint images collected from 200 unique finger instances captured in two different sessions. The database consists of subsurface fingerprints imaged at 6 different depth with Full-Field Optical Coherent Tomography (FF-OCT) resulting in a number of layers corresponding to depth of $70\mu m, 140\mu m, 210\mu m, 280\mu m, 350\mu m$ and $420\mu m$.
- Presents an extensive analysis on the newly collected FF-OCT fingerprint database to determine the suit-

ability of different layers of subsurface fingerprints to achieve reliable performance and recognition accuracy with a set of newly developed protocols.

- Presents a new framework based on estimated quality for fusing the FF-OCT image data from the set of images pertaining to different subsurface depth. Further, we present an analysis of the performance when different subsurface images are fused to obtain a single subsurface fingerprint.
- As a final contribution of this work, we evaluate applicability of cross-depth comparison accuracy for recognizing the subsurface fingerprint and thereby exploring the ability to compare various subsurface fingerprints. To the best of authors' knowledge, this is the first work to explore such a problem of matching subsurface fingerprints at various depths of imaging ($70\mu m, 140\mu m, 210\mu m, 280\mu m, 350\mu m$ and $420\mu m$).

In the rest of this paper, Section 2 presents the details of the custom built in-house FF-OCT sensor. Section 3 presents the details of the newly collected FF-OCT fingerprint database using the FF-OCT sensor. Further, Section 4 presents the detailed analysis of the database in terms of the biometric performance and Section 5 deduces the key observations and remark while listing the potential works in future.

2. FF-OCT Fingerprint Sensor

Schematics of the recently designed in-house FF-OCT sensor for acquiring the subsurface fingerprints is shown in Figure 2. The details of the system are presented in [3]. Briefly, it is comprised of an imaging interferometer, LED operating at $850nm$ and a silicon camera $Q-2A750-CXP, Adimec$. The camera was specifically designed for FF-OCT and thus, it has an unusually high full well capacity of $2\ million\ electrons$. A window is used to press a finger against such that the external layer is flattened and thereby reduce the involuntary motion and jitter during the time of capture. The FF-OCT sensor is able to record $1.72\ cm \times 1.72\ cm$ en face images in $0.12\ sec.$ with the spatial sampling rate of $2116\ dpi$ and sensitivity of $93\ dB$. Subsurface images at different depths were acquired by stepping the reference reflector between the images and the time it took to record 6 subsurface images was only $0.8\ seconds$.

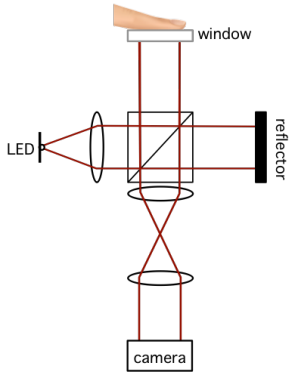

Figure 2: Schematic of the FF-OCT sensor. Spatially incoherent LED is collimated and injected into the imaging interferometer. Light reflected and scattered from a finger is imaged on the camera together with the reference beam. More details in [3]

3. Database

To demonstrate applicability and superiority of the recently designed sensor, fingerprint images from FF-OCT sensor was acquired from 200 unique fingers. The data was collected from the subjects in the age-group 20-40 years (including 3 people of age 70 years) who are typically not used to manual labour that may damage the external fingerprint. Further, the database was collected with a uniform ratio of male and female subjects. Each of the unique finger was captured in two different sessions resulting in a total of 400 images from 200 unique fingerprint instances. Each finger was imaged using the FF-OCT sensor resulting in 6 subsurface images that can be considered as 6 separate layers of $7.5\mu m$ thickness captured at the following depths: $70\mu m, 140\mu m, 210\mu m, 280\mu m, 350\mu m$ and $420\mu m$. Thus, the database consists of 6 images per-

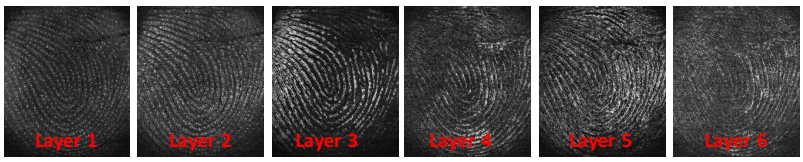

Figure 1: Sample fingerprint images captured at various subsurface depth using the FF-OCT device. The Layer-1 to Layer-6 corresponds to images acquired at the depth of $70\mu m$ to $420\mu m$ in the steps of $70\mu m$. The varying intensity across different layers can be noticed due to attenuation of the light by various tissues in the subsurface of the fingerprint. The lowest intensity can be observed in Layer-6 as most of the light is attenuated in the deepest imaging range corresponding to $420\mu m$.

taining to a particular fingerprint imaged at 6 different depth.

Figure 1 presents a sample fingerprint captured at 6 different depth below the surface starting from $70\mu m, 140\mu m, 210\mu m, 280\mu m, 350\mu m$ and $420\mu m$ represented by $Layer-1, Layer-2, Layer-3, Layer-4, Layer-5$ and $Layer-6$ respectively. It can be carefully observed from the Figure 1 that the details of subsurface image at different depth varies. The first layer presents a rich information of sweat ducts and fingerprint minutiae. The second layer presents the information very similar to the subsurface fingerprint at $70\mu m$ depth denoted by $Layer-1$ but the details of sweat-ducts diminish. As the depth of imaging is increased as indicated by $Layer-3$ and $Layer-4$ the strong pattern of internal fingerprint appears.

4. Experiments and Results

This section presents the experimental protocols and the obtained results from the newly collected database from the FF-OCT sensor. As the newly collected fingerprint database has two samples collected per fingerprint, one sample per fingerprint is used for enrolment and the other sample is used as probe. Further, in-order to fully leverage the database, we swap the reference and probe sample to obtain another set of scores. Thus, the total of number of genuine comparison scores equals to $200 \times 2 = 400$ while the number of impostor scores equals to $200 \times 199 \times 2 = 79600$. In this work, we employ VeriFinger Fingerprint SDK [13] to obtain the templates and to compare the templates as the software has to date been widely deployed in civilian applications. All results from the experiments in this work are reported in terms of False Match Rate (FMR %) and False Non-Match Rate (FNMR %) and represented in Detection Error Trade-off (DET) curves. Further, the Equal Error Rate (EER %) is also reported in similar terms.

As the sensor was only recently designed and correspondingly the database is newly obtained, we intend to evaluate the usability of different images pertaining to different depth in terms of biometric verification significance. Thus, we propose a new set of protocols to evaluate the FF-OCT subsurface fingerprint database as given below:

- Protocol-1 : Same Layer (Subsurface) Evaluation
- Protocol-2 : Fused Layer (Subsurface) Evaluation
- Protocol-3 : Cross Layer (Subsurface) Evaluation

4.1. Protocol-1 : Same Layer Evaluation

This set of experiments is designed to evaluate the robustness of subsurface images obtained from various depths from each finger instance. The main motivation for this protocol stems from the fact that the fingerprint information can be densely available or sparsely available depending on the depth of imaging ($70 - 420\mu m$ in our case). Added to that, the internal fingerprint can be at different depth for different fingers and also partially visible at a certain depth in a non-uniform manner as illustrated in the Figure 1. Thus, this set of experiments deduce the strength of various depth images to achieve good biometric performance. According to this protocol, image from a particular depth (say $Layer-1$) is enrolled from session 1 and the image from the corresponding depth ($Layer-1$) from session 2 is probed. Table 1 presents the set of results obtained by enrolling various layers from session 1 versus corresponding layers from session 2. The set of obtained DET curves can be seen in the Figure 4. As it can be deduced from the Table 1, following observations can be made:

- $Layer-2$ and $Layer-3$ corresponding to subsurface fingerprint provide very high accuracy (EER of 2.08% and 2.27% respectively).
- $Layer-6$ corresponding to the deepest imaged subsurface results in a high EER of 11.15%.
- Figure 3 presents the images and the corresponding features extracted. As it can be seen, the number of features extracted from $Layer-6$ is significantly lower than the number of features obtained in $Layer-1$ which can be attributed to the high EER obtained for images compared from $Layer-6$. Further, the subsurface image is not optimal since light absorption and scattering degrades image quality and SNR, as seen on the last row of the Figure 3.

4.2. Protocol-2 : Fused Layer Evaluation

As there is a number of layers available from the subsurface imaging of finger corresponding to different depth of imaging, one can fuse the information from various subsurface fingerprints to form a robust representation of the fingerprint with strong pattern and high Signal-to-Noise-Ratio (SNR). Thus, in this set of experiments, we form a fused subsurface fingerprint image by using the set of selected subsurface images on the basis of the overall fingerprint quality determined by Neurotech VeriFinger SDK [13]. Given a set of different images from $Layer-1$ to $Layer-6$ as given by $I = \{L_1, L_2, L_3, L_4, L_5, L_6\}$, we compute the quality factor for each image using the Neurotech VeriFinger SDK [13].

$$Q_i = Quality\{L_1, L_2, L_3, L_4, L_5, L_6\} \quad (1)$$

i represents the layer number or the depth of the subsurface image of a fingerprint corresponding to range $70\mu m, 140\mu m, 210\mu m, 280\mu m, 350\mu m$ and $420\mu m$. Based on the set of computed quality values from Neurotech VeriFinger SDK [13], we select three subsurface images resulting in a high quality value as given by:

$$\{L_{q1}, L_{q2}, L_{q3}\} \leftarrow \arg\max\{Q_1, Q_2, \ldots Q_6\} \quad (2)$$

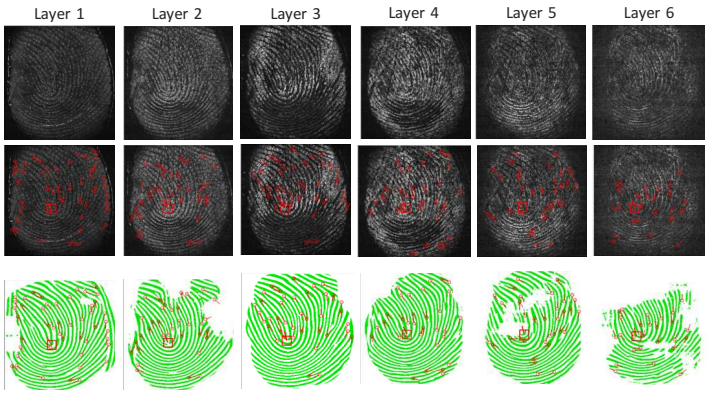

Figure 3: Illustration of minutiae template extraction from VeriFinger SDK [13] across 6 different layers of a fingerprint corresponding to different depths of imaging (Layer-1 corresponds to subsurface image at $70\mu m$ and Layer-6 corresponds to subsurface fingerprint at $420\mu m$). Top row presents the image data from different depth and bottom rows depict the features extracted and overlaid on fingerprint. The bottom most row presents the fingerprint in binary template and the extracted features overlaid. It can be observed that the number of minutiae diminishes as deeper fingerprints are imaged.

Table 1: Verification performance obtained for Protocol-1 and Protocol-2.

Protocol	EER (%)					
	Layer-1	Layer-2	Layer-3	Layer-4	Layer-5	Layer-6
Layer v/s Layer	2.57	**2.08**	3.00	2.27	6.24	11.15
Fused Layer v/s Layer	2.07	1.72	1.44	**0.93**	2.14	3.08
Fused Layer v/s Fused Layer	**0.00**					

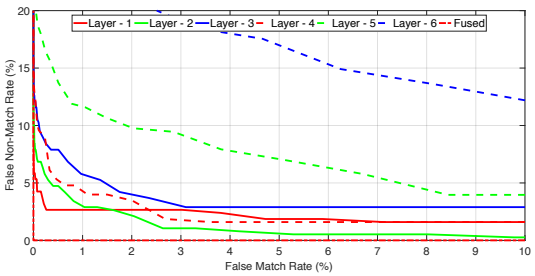

Figure 4: Verification performance of fingerprint samples obtained at various depth of imaging.

The layers denoted by $\{L_{q1}, L_{q2}, L_{q3}\}$ represent the selected layers according to maximum quality values represented as $q1, q2$ and $q3$. The selected subsurface images are further provided to Neurotech VeriFinger SDK [13] to generate the generalized template with the proprietary fusion algorithm. The obtained image with all the chosen subsurface images fused is employed to extract the template. The template obtained from the fused subsurface image is compared against the template extracted from independent subsurface images. Thus, in this protocol, we conduct two experiments where fused subsurface fingerprints from session 1 is compared against different subsurface images from session 2. In the second set of experiments, the fused subsurface image from session 1 is compared against the fused subsurface image from session 2. The results obtained from this set of experiments are presented in the Table 1. The key observations and remarks from this set of experiments are listed below:

- Comparing the fingerprint template from fused subsurface images of session-1 against the subsurface image corresponding to $Layer - 4$ of session 2 yields a very low EER (0.93%) indicating the efficiency of the fusion approach.
- A significant gain can be observed in comparing the image from $Layer - 6$ against the fused image where a relative reduction of 72% can be seen with an obtained EER of 3.08%. The obtained EER signifies the importance of the template based on the fused image to compare against fingerprint from different depth of subsurface layer.
- In the second set of experiments where the fused image from session 1 is used to extract the template and compared against the template from fused image of session

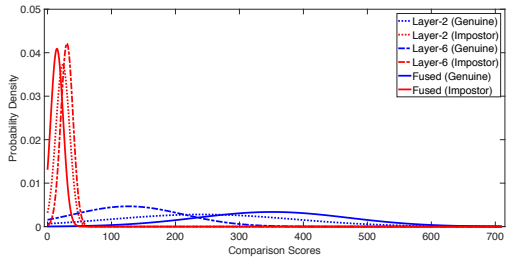

Figure 6: Distribution of comparison scores at various depth of imaging

2, an EER of 0% is achieved. The corresponding DET curve can be seen in the Figure 4 where the superior performance is evidently seen. Along the similar lines of observation, the probability density function of the genuine and impostor scores indicate the zero overlap for the fused image template comparison as depicted in Figure 6.

- Figure 5a presents the significance of the fused subsurface approach where the median value of genuine scores is much higher than the scores obtained from $Layer\ to\ Layer$ template comparison. Specifically, the genuine scores are clearly higher as compared to genuine scores obtained for comparisons of $Layer - 4, Layer - 5$ and $Layer - 6$. In the similar terms, Figure 5b presents the box-plot of the impostor scores across different layers of comparison and it can be observed that the impostor scores are significantly reduced justifying the higher gain in the performance of with the proposed fusion approach.

Further, to obtain the fused templates, the quality threshold of the Neurotech VeriFinger SDK [13] was set to 0 without which a number of subsurface fingerprint images were rejected. This can mainly be attributed to the fact that the Neurotech VeriFinger SDK [13] is tuned to optical fingerprints as compared to FF-OCT fingerprints.

4.3. Protocol-3 : Cross Layer Evaluation

Table 2: Verification performance obtained for Protocol-3

Note - The distance between templates is not symmetric and thus, there is a small difference in EER when two different layers are compared in reversed order.

Protocol	EER (%)					
	Layer-1	Layer-2	Layer-3	Layer-4	Layer-5	Layer-6
Layer-1	**2.57**	2.73	4.50	5.70	10.13	14.78
Layer-2	2.79	**2.08**	4.17	7.41	11.40	14.18
Layer-3	4.08	4.28	**3.00**	6.48	10.30	15.36
Layer-4	5.36	7.21	5.48	**2.27**	7.49	14.61
Layer-5	10.21	10.65	10.58	7.66	**6.24**	13.85
Layer-6	14.89	13.89	17.25	14.73	13.82	**11.15**

The experiments in this protocol are mainly designed to gauge the robustness of subsurface fingerprint comparison across different depths of imaging. This protocol is particularly relevant on the following arguments:

- When the external fingerprint is damaged due to minor injuries due to abrasions, cuts or burns, the subsurface fingerprint can be employed to recognize individuals with undamaged subsurface fingerprints. As the information from a subsurface fingerprint is minimally disturbed under the above mentioned conditions, it is essential to determine the suitability of the images at different depth and to compare against the previously acquired (before external damage) image. Further, it has to be noted that the details observed in a subsurface fingerprint are directly impacted by the depth of imaging. Thus it is essential to measure the reliability of subsurface fingerprints for biometric performance and thereby, we measure the biometric performance across the different depth of subsurface imaging ranging from $70\mu m$ to $420\mu m$.
- As OCT images can be used to determine the liveness of the presented fingerprint, in accordance to general physiology, subsurface layers should be minimally shifted if not exactly aligned. Thus, any subsurface

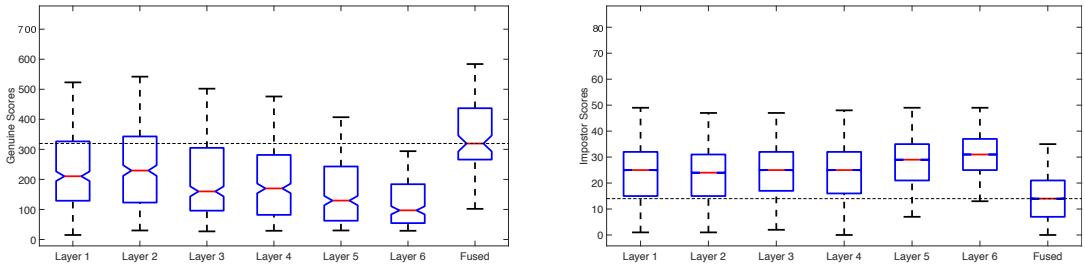

(a) Genuine scores

(b) Impostor scores

Figure 5: Comparison of genuine and impostor scores across different depth of imaging along with the scores from fused template.

fingerprint exhibiting the anomaly at different depth can aid in detecting presentation attacks. Alternatively, analysing the comparison scores amongst the set of subsurface images could potentially indicate the liveness.

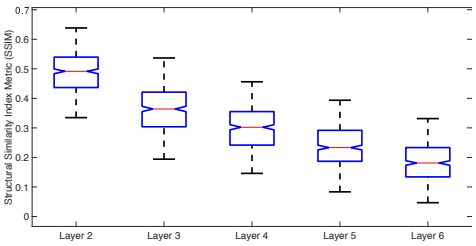

Figure 7: Structural similarity index measured across different layers with Layer-1 being the reference.

In order to meet the goals mentioned above, it is essential to first measure the reliability provided by multiple subsurface images in fingerprint. Thus, in this protocol, we enrol the image from session 1 corresponding to a particular subsurface (layer), say $Layer - n$ and probe all the fingerprint images relating to other layers/subsurface. For instance, $Layer-1$ is enrolled and $Layer-2$ to $Layer-6$ are compared. Table 2 presents the verification performance in terms of EER for various cross-layer evaluation and Figure 8 presents the DET curves obtained when the enrolment image is changed to different layers and probed against the number of other layers. The key observations are listed as below:

- The comparison of templates from $Layer - 1$ to $Layer - 2$ result in lowest error rates ($< 3\%$) as the subsurface fingerprint are highly correlating. The quality of subsurface fingerprint images from the two layers are not significantly degraded by light absorption and scattering in a finger and thereby templates are matched with high scores.
- Figure 3 presents a sample illustration of the features extracted from different layers of image corresponding to different depth in the fingerprint. As it can be seen, the number of features obtained in $Layer-1$, $Layer-2$ and $Layer-3$ are high in number and stable in terms of locations.
- It can also be noted that the EER increases as the separation between the layers increases resulting in subsurface images of depths with very few patches correlating. The key reasons for this can be attributed to the change of the appearance of a subsurface fingerprint with the increasing depth [3] as well as increase in image degradation due to the light absorption and scattering. The lower similarity among the subsurface layers is quantitatively measured using Structural Similarity Index Metric (SSIM) by considering the subsurface image at depth of $70\mu m$ as reference and the obtained scores are presented in Figure 7. From the figure, it can be noted that the structural similarity decreases as the depth of the subsurface fingerprint images increases due to the change in the anatomy and image degradation.
- The comparison between $Layer - 6$ and $Layer - 3, Layer - 1$ increases the EER by a magnitude of order 5x (2.57% to 15.36%) as compared to EER obtained between $Layer - 1$ for instance.

5. Conclusions and Remarks

With the growing concern for presentation attacks against biometric systems and the need for resistant and fool-proof fingerprint capture devices with the ability to handle minor external injuries on fingerprint, a new generation of sensors based on Optical Coherence Tomography has shown promising results. The ability to image the subsurface fingerprint by the use of full field optically coherent tomography sensor has been demonstrated to detect artefacts and to handle minor changes in external pattern by capturing the subsurface fingerprint. In this work, we have presented a new fingerprint database collected using FF-OCT sensor with 200 unique finger instances with 6 layers pertaining to various depth of imaging. An extensive analysis of the fingerprint database was presented and key observations were listed in the corresponding sections (refer Section 4). Further, we have also presented a new approach of fusing the layers corresponding to various depth of images which is further used to extract robust templates for comparison. In the first set of experiments, we have shown the performance of independent layer of fingerprint images using a commercial-off-the-shelf SDK from Neurotechnology such that the significance of each layer is established. Further we have demonstrated the applicability of the proposed approach of fusion by experimentally validating the superior performance resulting in $EER = 0\%$. As a final contribution, we have evaluated the cross-layer fingerprint comparison where the different subsurface fingerprint image is compared against other subsurface fingerprints images at various depth bringing out the observation on relevant subsurface depth for accurately verifying the subjects.

As a set of conclusive remarks, this work lists the following observations and future works:

- The promising nature of FF-OCT fingerprint imaging has been experimentally validated by a set of extensive experiments with newly collected fingerprint database of 200 unique fingerprint images. Each of the fingerprint collected in less than 1 second has 6 layers of subsurface fingerprints capturing sweat ducts inside the stratum corneum and a fingerprint pattern inside the

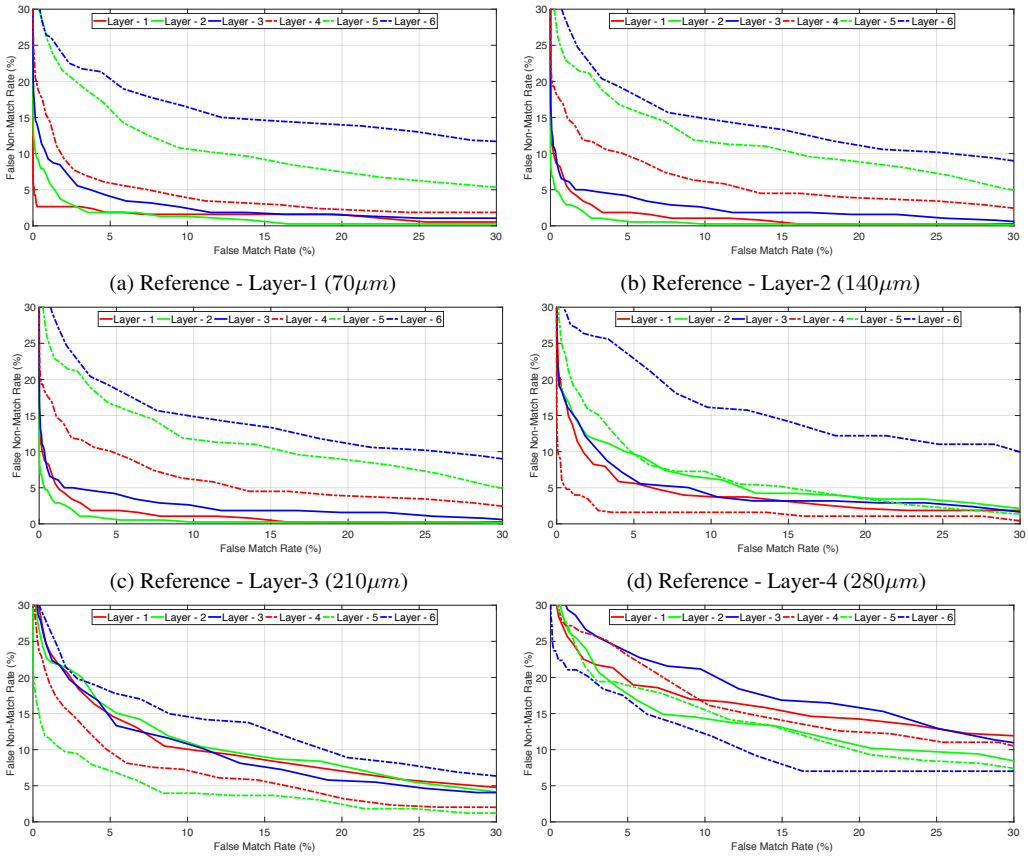

(a) Reference - Layer-1 ($70\mu m$)

(b) Reference - Layer-2 ($140\mu m$)

(c) Reference - Layer-3 ($210\mu m$)

(d) Reference - Layer-4 ($280\mu m$)

(e) Reference - Layer-5 ($350\mu m$)

(f) Reference - Layer-6 ($420\mu m$)

Figure 8: Performance obtained when different layers corresponding to different depth are enrolled while rest of the images from other depth are probed.

stratum corneum and from the viable epidermis (otherwise know as internal fingerprint) collected in two different sessions.

- The obtained accuracy of $EER < 2.5\%$ for fingerprint images $Layer-1$, $Layer-2$ and $Layer-3$ signify the usability of subsurface imaging using FF-OCT to obtain reliable biometric performance. With the proposed image fusion approach, the recognition accuracy is further improved by attaining an EER of 0.93% by comparing the fused image template against $Layer-4$. An accurate classification has been demonstrated by using the fused image template at both reference and probe part resulting in $EER = 0\%$. The clear difference in the score distribution has been illustrated with the fused image approach as depicted in Figure 5.
- The cross-layer verification indicates the challenging nature due to availability of partial internal fingerprint in the subsurface layers (it might be curved despite the fact that the external (surface) fingerprint is flat). Comparing the fingerprint pattern imaged from deep layers against corresponding layers results in $EER = 11\%$ and comparing them against the lower depth subsurface fingerprint ($70\mu m$) results in an $EER = 15\%$ (refer Table 2).
- It has to be noted that the current work has employed the database with fairly large size of 200 unique fingerprint images and the results come with the caveat to study on a larger group, ethnicity and number of different sessions to validate the findings derived from this work.

Acknowledgements

This research was conducted in the scope of the INGRESS project, funded by the European Unions Seventh Framework Programme for research, technological development and demonstration under grant agreement no 312792.

References

[1] A. Alex, B. Považay, B. Hofer, S. Popov, C. Glittenberg, S. Binder, and W. Drexler. Multispectral in vivo three-dimensional optical coherence tomography of human skin. *Journal of biomedical optics*, 15(2):026025–026025, 2010. 2

[2] E. Auksorius and A. C. Boccara. Fingerprint imaging from the inside of a finger with full-field optical coherence tomography. *Biomedical optics express*, 6(11):4465–4471, 2015. 1, 2

[3] E. Auksorius and A. C. Boccara. Fast subsurface fingerprint imaging with full-field optical coherence tomography system equipped with a silicon camera. *arXiv:1705.06272*, 2017. 2, 3, 7

[4] J. Aum, J.-H. Kim, and J. Jeong. Live acquisition of internal fingerprint with automated detection of subsurface layers using oct. *IEEE Photonics Technology Letters*, 28(2):163–166, 2016. 2

[5] A. Bicz and W. Bicz. Development of ultrasonic finger reader based on ultrasonic holography having sensor area with 80 mm diameter. In *Biometrics Special Interest Group (BIOSIG), 2016 International Conference of the*, pages 1–6. IEEE, 2016. 1

[6] A. Bossen, R. Lehmann, and C. Meier. Internal fingerprint identification with optical coherence tomography. *IEEE photonics technology letters*, 22(7):507–509, 2010. 2

[7] Y. Cheng and K. V. Larin. Artificial fingerprint recognition by using optical coherence tomography with autocorrelation analysis. *Applied optics*, 45(36):9238–9245, 2006. 2

[8] I. Grulkowski, J. J. Liu, B. Potsaid, V. Jayaraman, A. E. Cable, and J. G. Fujimoto. Ultrahigh speed oct. *Optical Coherence Tomography: Technology and Applications*, pages 319–356, 2015. 1

[9] F. Harms, E. Dalimier, and A. C. Boccara. En-face full-field optical coherence tomography for fast and efficient fingerprints acquisition. In *SPIE Defense+ Security*, pages 90750E–90750E. International Society for Optics and Photonics, 2014. 1

[10] E. H. Holder, L. O. Robinson, and J. H. Laub. *The fingerprint sourcebook*. US Department. of Justice, Office of Justice Programs, National Institute of Justice, 2011. 2

[11] G. Liu and Z. Chen. Capturing the vital vascular fingerprint with optical coherence tomography. *Applied optics*, 52(22):5473–5477, 2013. 2

[12] M. Liu and T. Buma. Biometric mapping of fingertip eccrine glands with optical coherence tomography. *IEEE Photonics Technology Letters*, 22(22):1677–1679, 2010. 2

[13] Neurotechnology. VeriFinger SDK. 4, 5, 6

[14] R. Rowe, K. Nixon, and P. Butler. Multispectral fingerprint image acquisition. *Advances in biometrics*, pages 3–23, 2008. 1

[15] C. Sousedik, R. Breithaupt, and C. Busch. Volumetric fingerprint data analysis using optical coherence tomography. In *Biometrics Special Interest Group (BIOSIG), 2013 International Conference of the*, pages 1–6. IEEE, 2013. 1

[16] X. Yu, Q. Xiong, Y. Luo, N. Wang, L. Wang, H. L. Tey, and L. Liu. Contrast enhanced subsurface fingerprint detection using high-speed optical coherence tomography. *IEEE Photonics Technology Letters*, 29(1):70–73, 2016. 1

[17] A. Zam, R. Dsouza, H. M. Subhash, M.-L. O'Connell, J. Enfield, K. Larin, and M. J. Leahy. Feasibility of correlation mapping optical coherence tomography (cmoct) for anti-spoof sub-surface fingerprinting. *Journal of biophotonics*, 6(9):663–667, 2013. 2